



## Research Article

# Experimental study of heat transfer in a helical coiled tube biomass fired rotary device

Prashant DESHMUKH<sup>1\*</sup>, Satyajit KASAR<sup>2</sup>, Niteen SAPKAL<sup>3</sup>

<sup>1</sup>Department of Mechanical Engineering, College of Engineering Pune (CoEP), Pune-411005, Maharashtra, India

<sup>2</sup>Department of Mechanical Engineering, Sandip Institute of Technology and Research Centre, 420003, Nashik, India

<sup>3</sup>Department of First Year Engineering, Pune Institute of Computer Technology, 410014, Pune, India

## ARTICLE INFO

### Article history

Received: 25 January 2021

Accepted: 11 June 2021

### Keywords:

Biomass; Bagasse; Helical Coiled Tube Flow; Rotary Combustion Chamber

## ABSTRACT

The present investigations put forth the development of a novel double wall vented rotary fluid heating device. In this device, water is used as a process fluid and is heated by the combustion of sugarcane bagasse. The proposed combustion method is found to provide the use of a more systematic fuel transport system and ensure the efficient heat transfer process to the fluid. It is observed to offer many advantages over the conventional furnaces and obviates the use of any mechanized system such as traveling grate, fluidized bed system, dumping grate, etc. in conventional systems. Also, the heat liberated in combustion is used effectively for heating fluid through a helical coiled tube mounted over the surface of the drum. The present study aims to assess the thermal performance of the proposed rotary combustion chamber at different experimental parameters. It was concluded to have a maximum temperature rise, and the thermal efficiency of this system at 45.3C and 45.2% when drum speed is 6 RPM at Reynolds number equal to 1176.

**Cite this article as:** Deshmukh P W, Kasar S V, Sapkal N P. Experimental study of heat transfer in a helical coiled tube biomass fired rotary device. J Ther Eng 2022;8(6):772–785.

## INTRODUCTION

Biomass is one of the promising renewable energy resources, and presently supplies an energy need in the rural and underprivileged sectors. It is derived from numerous sources, including by-products from the timber industry, crops, raw material from the forest, and major parts of household waste [1].

Different types of biomass can be grown for the express purpose of energy production. Crops that have been used for energy production include Sugarcane bagasse, Wheat straw, Rice hulls, Corn, Sugar beets, Kelp (seaweed), and many others. Biomass is a sustainable fuel that can deliver

\*Corresponding author.

\*E-mail address: [pwd.mech@coep.ac.in](mailto:pwd.mech@coep.ac.in)

This paper was recommended for publication in revised form by Regional Editor Younes MENNI



a significant reduction in net carbon emissions when compared with other fossil fuels. The conversions of carbon-to-carbon dioxide or carbon monoxide etc. are the prominent issues associated with the burning of such kinds of fuels. However, the production and use of these as fuel are being carried out in a very unsustainable manner. The proper technical methodology and processes can lead towards the effective use of biomass fuel and have the potential to be as effective as conventional fuels. Furnaces for the combustion of these biofuels have been in use for a long time. These are developed with concepts parallel to those used for the combustion of coal or wood although the fact remains that these are low carbon content fuels. Biomass available in large quantities in rural, semi-urban, and urban areas, is the best suitable fuel and has the potential to fulfill this future requirement for maintaining the carbon cycle [10]. Therefore, there is a need for such a device that can ensure the complete and satisfactory combustion of biomass. The heat of combustion released from biomass if well harnessed can be utilized for heating water or any other process fluid in food processing industries, hotels, laundries, small paper industries, textile industries set in the rural areas, and also for general domestic purposes.

The present study aims to examine the use of advanced fuel transport and thermally efficient systems using bagasse, a refused material after crushing sugar cane. Comprehensive guidance about the methodologies, equipment, and processes concerning sugar cane is documented by Hugot [1]. Vertical cyclone furnaces, cyclone injection firings, sloping grate firings, combined grate/coal dust firings, or fluidized bed firing installations are few conventional combustion methodologies that have been reported in the literature extensively. Berdowski *et al.* [2] investigated the vertical cyclone furnaces which are modern low-emission installations for the combustion of wood with the thermal output of approximately 800 kW. Here, the design makes the air blow for combustion tangentially into the combustion compartment in order to achieve a thorough admixture and a high dwell time of the firing gases in the combustion compartment. Another design of cyclone furnace developed by Teir *et al.* [3] showed a narrow base in which secondary air is injected into the cyclone. It induces a strong swirl which causes a movement of large coal/char particles towards the furnace walls. Another air stream, called tertiary air, controls the position of the main combustion zone which is the primary source of radiant heat. Cyclone-fired boilers are used for coals with a low ash fusion temperature, which is difficult to use with a Pulverized Coal Fired (PCF) boiler. In such designs, 80-90% of the ash leaves the bottom of the boiler as a molten slag, thus reducing the load of fly ash passing through the heat transfer sections to the precipitator or fabric filter to just 10-20% of that present. The authors reported that the cyclone firing method can be used successfully to fire brown coal i.e. Lignite which is an inferior quality owing to

its high ash content and lower calorific values. Moreover, in comparison with the flame of a conventional burner, this methodology of combustion provides high-intensity, high-velocity cyclonic flames. This contributes to make heat transfer more effective to water-filled tubes, resulting in the unusual combination of a compact boiler size and high efficiency. However, the severe drawback of the cyclone firing method is a narrow operating temperature range of 600°C to 900°C. Besides this, there is an ash removal system for the furnace. Gluszynski *et al.* [4] reported the concept of a sloping grate furnace for the use of wood shavings as fuel. The combustion compartment was preheated by an ignition burner up to the operating temperature before being switched over to firing the wood shavings. The boiler temperatures were observed to be in the range of 700°C to 1000°C. The use of a moving grate furnace was especially intended for municipal waste incineration. The construction of the grate enables the moving of all its parts which allows mixing of waste and appropriate access to air. The temperatures in these furnaces observed were in the range of 850°C-1000°C. Three types of moving grate furnaces have been tested, firstly the Martin system in which the grate of the furnace has the reciprocating movement of the burning waste back to the loading zone. This further ensures burning waste mixing with the fresh fuel for thorough drying. The grate size is usually large enough for rapid cooling of residue incineration automatically falls into the slug receiver for use in the next cycle. Another moving grate furnace is the Düsseldorf system in which the grate is composed of sloping rolls, or drums, arranged in a cascade-like way. The waste is slowly turned and shifted, falling from one drum onto another. Flue gases move in the direction opposite to the movement of the waste for drying purposes and then light gases are ignited. Additionally, to regulate the combustion process, and to have cooled off the grate, the air blows below the grate. The system allows to modify of the air intake for each drum separately. The Von Roll combustion chamber system depends on the several grate blocks arranged in a cascade. In this arrangement, the waste is loaded on the feeder first, and then pushed on the drying grate, further over to the combustion grate; slug and ash fall upon a post-combustion grate. The last grate is equipped with a poker that rakes the slug and allows light ash to separate so that it can be post-combusted. The fluidized bed furnace having a shape of a vertical cylinder covered with heat-resisting material has been reported. This furnace is utilized to destroy sediments and solid or liquid waste of the same or similar composition, size, and energetic value. The furnace is also equipped to destroy some sorts of industrial waste or to incinerate Refuse Derived Fuel (RDF) which is produced from the pressed homogenous municipal waste or daily use items discarded by people. The air that ensures swelling and fluidization of the sand bed up to 100% of the primary volume, is pumped after preheating, under the pressure of 0.2-0.3 atm through a nozzle at the bottom

of the furnace. The waste is mixed with the sand or it is loaded from the upper part of the furnace. The temperature of the bed is limited by the temperature of the slag melting point and it is not higher than 1000°C. The methodology of combustion for the rotary furnace is reported by authors [4] for destroying industrial and toxic wastes in the form of the liquid phase, gas products of organic processes, sludge, paste, and solid combustible substances. A cylindrical container covered with heat-resisting material rotates around a slightly inclined horizontal axis with a speed of 1-5 rpm. The solid waste is loaded at the higher end of the cylinder and it slides down inside the container. Liquid waste and the additional fuels are injected into the main chamber or the secondary ones. Additional burners are used to ignite and support the combustion of organic substances. Gases arising during the process travel from the first chamber to another in a post-combustion chamber. The temperature in the rotary furnaces is likely to be 1300°C, however, it may reach 1600°C. Gluszynski *et al.* [4] also reported the working of shelf furnaces that are suitable to incinerate waste with a large content of water. Like other rotary furnaces, they are cylindrical in shape, covered with the heat-resisting material, mounted with 4 to 14 numbers of horizontal shelves at the inner portion. The construction of each shelf facilitates the pushing of the waste from the loading zone to the place from where the waste is dumped on the following shelf and then to the point at which the ash is unloaded. This method ensures drying of the waste, its combustion process, and, finally cooling of the ash. The combustion products and air are moving counter-current, to the movement of the waste. The shelf furnaces are more efficient when working continuously as their start-up may require a long time up to 24 hours. The temperature in

the combustion chamber is around 1000°C, which is the temperature of the slag melting point, demanding a large amount of excess air.

Leland and William [5] used a rotary combustion apparatus as shown in Fig.1 which consist of a cylindrical drum, or other similarly shaped chambers, with a principal combustion horizontal axis of rotation including an ignition zone, a principal combustion zone, a falling temperature zone and spent solid removal zone. Transport chutes are placed for the transfer of solids to or from one or more points for forward and backward circulation. This apparatus ensures the direct solids-to-gas contact by lifting and cascading combustible solids through a hot gas stream. The apparatus is used for combustible solids, liquids, or gases, such as sewage sludge, refuse, coal, refinery sludge, tar sands, coal tailings, and spent foundry sand. The apparatus contains solid transport chutes for forward and backward circulation of solids, arranged for the transfer of solids to or from one or more points. Like earlier apparatus, this method also employs direct solids-to-gas contact established by lifting and cascading combustible solids through a hot gas stream.

Larson and Branscome [6] reported an apparatus for the combustion of tires in a horizontally rotating enclosure. The tires are loaded into a rotating combustion chamber through a traveling airlock and burnt until reduced to ash. The combustion process is enhanced by tumbling the burning tires in the rotating chamber while adding preheated draft air. The apparatus is so designed to control the intake draft of air through the draft control valve. The inner surface of the chamber is tapered to prevent unburnt debris from advancing prematurely; however, angled flights, positioned along the inner surface, cause the residual ash to advance with

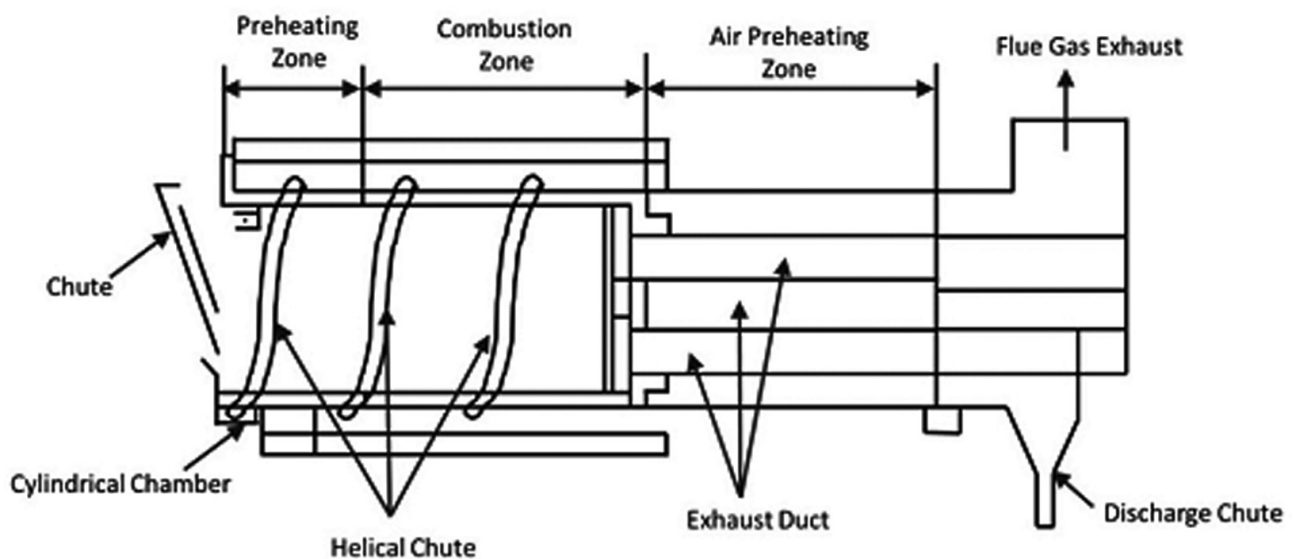
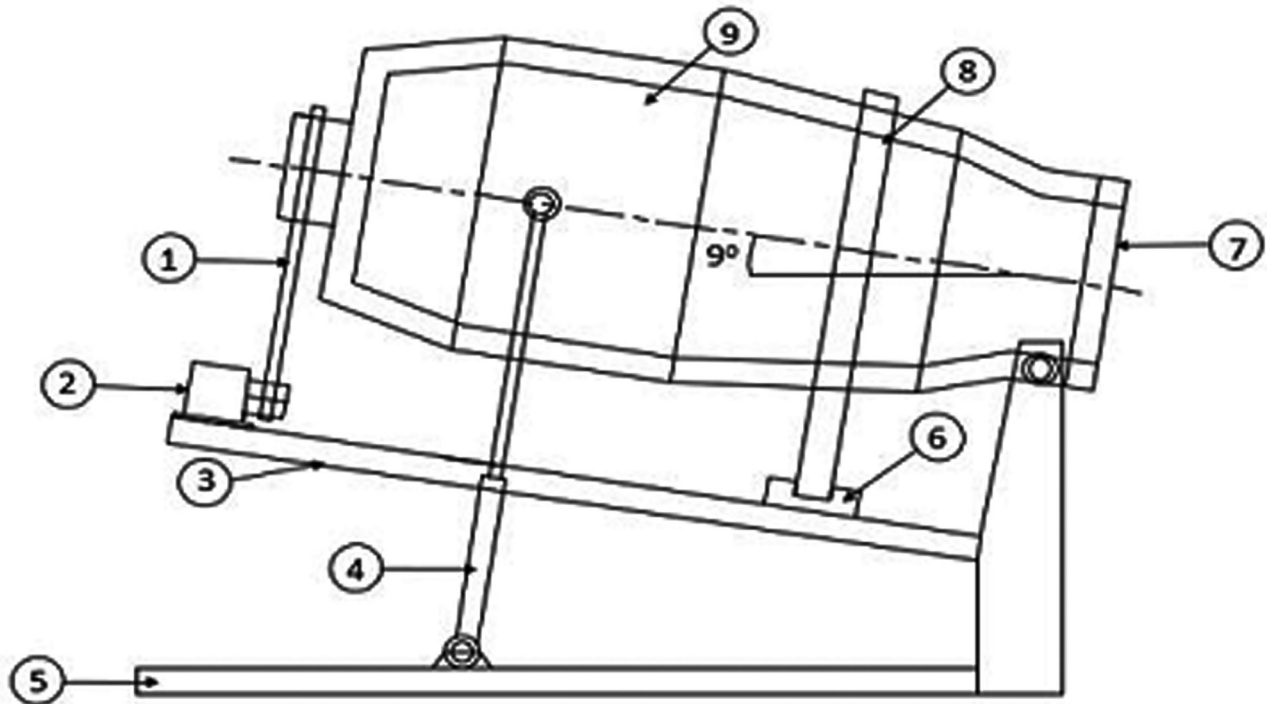


Figure 1. Apparatus for the Combustion of Diverse Material.



- |                       |                  |                         |                              |
|-----------------------|------------------|-------------------------|------------------------------|
| <b>1. Chain Drive</b> | <b>2. Motor</b>  | <b>3. Platform</b>      | <b>4. Hydraulic Cylinder</b> |
| <b>5. Base</b>        | <b>6. Roller</b> | <b>7. Mouth of Drum</b> | <b>8. Drive Ring</b>         |
|                       |                  |                         | <b>9. Drum</b>               |

Figure 2. Swivel-based tilting rotary furnace [7].

each successive revolution of the combustion chamber. The resultant combination of gases and ash is then forwarded to an afterburner for the completion of combustion and disposal of the ash. Mansell [7] has patented a swivel-based tilting rotary furnace for recycling metal, shown in Fig.2. This design concept forms a basis for the rotary device used in the present study.

The furnace comprises of a hollow elongated drum having a tapered snout, a door closing the front opening, a power rotary drive to rotate the drum which is mounted for tilting about the transverse axis, and for swiveling about a vertical axis and a heater. The recycling of the metal is achieved by melting the metal to remove it from the metal-containing scrap through the use of a tiltable which is swiveled to a first station for receiving metal-containing scrap, tilted back, and rotated while heating to melt the metal. Then the tiltable section is further swiveled and stopped to a second station and forward-tilted to quickly pour off molten metal into the holding apparatus. The furnace is swiveled to the third station where it is further forward-tilted and rotated to discharge the residual scrap and then leveled and swiveled to the first station for the next set of the cycle. This sequence of operations occurs in a quick time which

results in the reduction of the amount of energy required to reheat the furnace.

Swithenbank [8] has patented a rotating fluidized bed incinerator. It comprises a rotating combustion chamber, a mechanism for rotation and loading of combustible material into the combustion chamber, and the arrangement of introducing a gas into a combustion chamber to create a fluidized bed. The process occurs in a particular sequence which results in a reduction in the combustion time and loss of heat energy to the ambient. The advantage of fluidized bed combustion can be taken to introduce lower calorific value fuels such as biomass for consumption.

A thermodynamic study for a fluidized bed combustion system of a power plant using coal as a fuel is put forward by Tantekin1 and Özdil [9]. The use of the 1<sup>st</sup> and 2<sup>nd</sup> laws of thermodynamics can be seen. The authors reported that the fluidized bed coal combustion system that miscarriage calorific value, excess air in the combustion chamber, affect the effectivity of the plant, also excess oxygen contents causes temperature drop and it further reduces combustion efficiency. The optimum value of excess air needs to be provided for the high thermal efficiency of the plant has been also worked out.



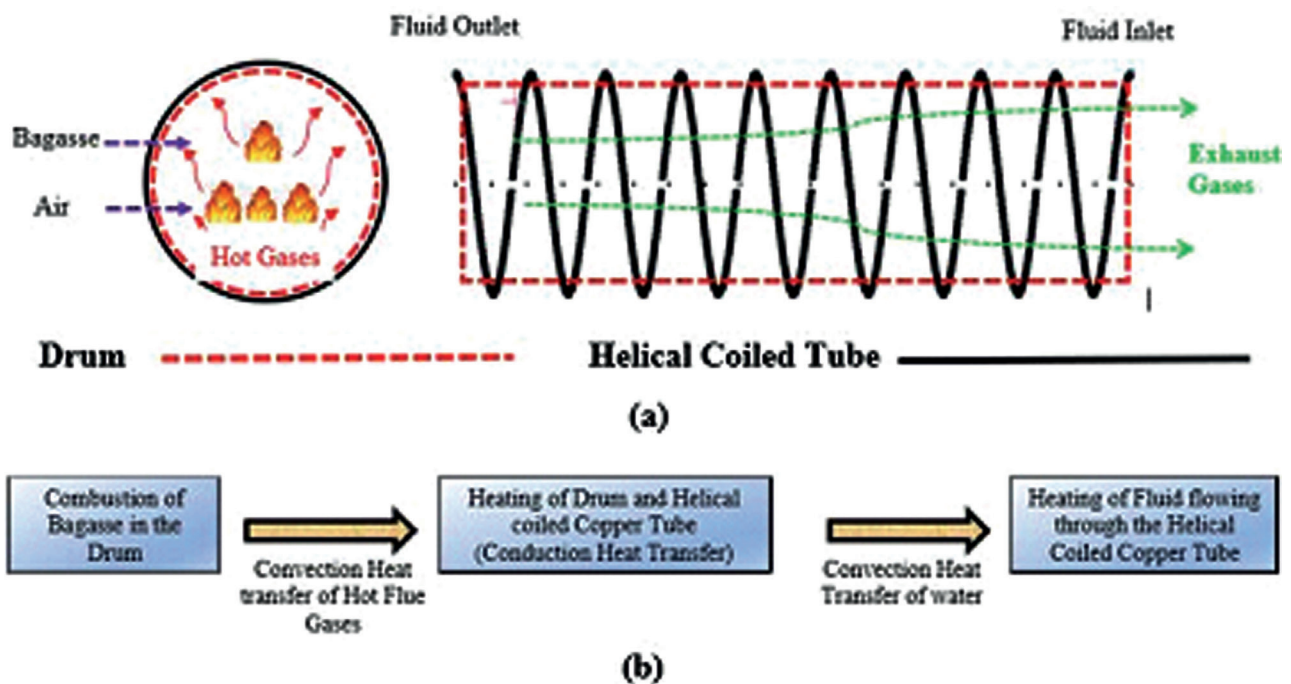


Figure 3. (a) Process Flow (b) Sequence of Process.

Mehrabian *et al.* [10] reviewed literature extensively for numerical studies available for biomass grate firing systems to adopt a new design for the reduction in emissions, and for enhancement of overall efficiency. The recent technologies with respect to fuel bed thermal combustion, gas-phase combustion, pollutant formation and their emissions, and the optimization procedure are reported. The authors emphasize the need for experimental investigations on biomass grate furnaces for effective and efficient energy extraction.

There has been the application of tilted rotary furnaces proposed in the casting of metals [11]. Its prime task is to provide a melting chamber. The metal enters through the inlet door and enters into the graphite chamber. The fuel used is propane gas for heating the metal. The furnace rotates through complete  $360^\circ$  and the tilt angle can be controlled through external gears. The designers have claimed in the reduction of manufacturing cost due to reduction in the wastage. In one of the research on reduction in  $\text{NO}_x$  in pulverized boilers, the principle underlying the imparting oscillatory motion is to interrupt fuel or part of the combustion air to change the local stoichiometry [12]. When compared with stationary or full rotational combustion chambers, the rate of reduction could reach 50%.

In the literature review, it is observed that there is a limitation for the existing combustion chambers to handle proper combustion of bagasse. Also, there is a lack of appropriate technical process necessary which can result in the effective use of biomass fuel. In the present study,

with respect to the flow regime bound for the experimental work, the appropriate correlation for friction factor is used to estimate the pressure drop expected in the particular flow regime. In this regard, Shaukat Ali's collection of work [13] has been of great use to establish the correlations for pressure with respect to the mass flow rate. The helical coiled circular tubes of six configurations of different coil diameters, pitch, and the number of turns were designed. The author presented the experimental data in terms of dimensionless parameters i.e. Euler number and Reynolds number. Hardik *et al.* [14] reported the experimental study of flow through the helical coiled tube, and the effects of curvature, and Reynolds number on local heat transfer coefficient. The authors concluded that the helical coil tube can minimize the thermal expansion of tube material due to the generation of secondary flow within the tube compared to a straight tube, especially at high-temperature applications. The authors also reported a brief literature review on the flow through the helical coiled tube and reported correlations for average as well as local Nusselt number at inner and outer sides and at the total surface of a helical coil.

The research so far reviewed set the tone to move towards the primary objective of the study which is to improve the combustion process for biomass in general and bagasse in particular. In the present study, an experimental investigation on a novel double wall vented biomass-fired rotary device is carried out. The proposed rotary heating device obviates the use of additional mechanisms used in conventional combustion devices and aimed to work

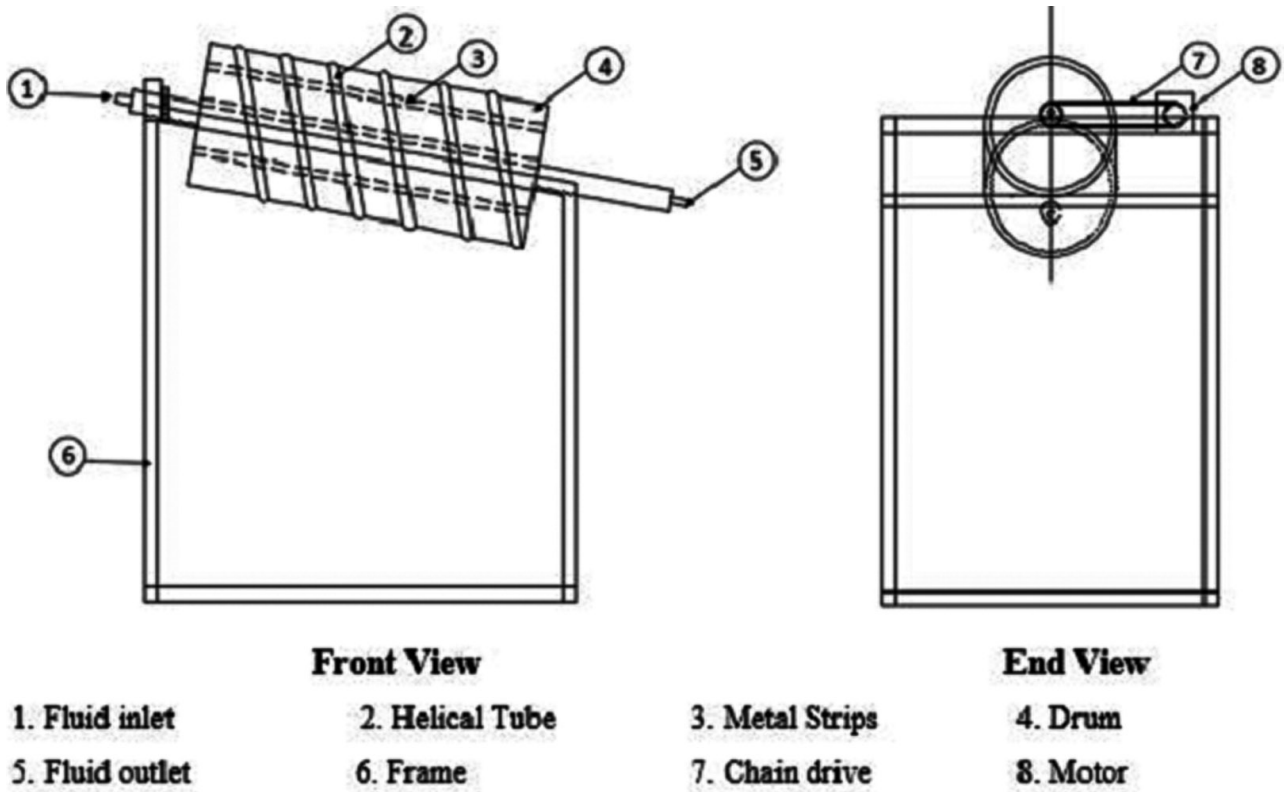


Figure 4. Conceptual Design of Experimental Setup.



Figure 5. Photograph of Experimental Setup.

without any special conveyor and ash handling systems to continuously heat the fluid. Further, the fluid, which is to be heated, is allowed to pass through a helical coiled circular tube brazed over the combustion chamber drum. The helical wire-coiled circular tubes have a large heat transfer area within a small space in comparison with the straight circular pipes.

The structure of the paper includes an introduction, conceptual design and methodology adopted, experimentation,

estimation of pressure drop for flow through a helical pipe, the results are analyzed and subsequently, a comprehensive conclusion is presented which further throws light on the future scope of the present study.

**CONCEPTUAL DESIGN AND METHODOLOGIES**

The configuration of the proposed rotary fluid heat-ing device originated through the study of the concept used in Mansell’s patented design of a swivel-based tilt-ing rotary furnace [7]. Also, the configuration of transport helical chutes used in the rotary drum for the heat trans-fer by Leland and Leland and William [5] helped to shape the thought process which finally culminated into a helical tube welded over the drum. A process sequence is shown in Fig.3, which is consisting of the generation of hot flue gases in the combustion chamber, shown by a horizontal dashed rectangle for presentation purposes only, The heated helical coiled copper tube shown by solid lines, through the conduction heat transfer process, and then heating of flowing water through it by convection from the inner tube surface.

The process starts at the combustion of bagasse in the rotary drum. The slow oscillatory rotary motion of the drum causes thorough mixing and ensures the supply of required air for the combustion process. The convection of

air inside the drum, and some form of direct heating causes the inner part of the drum to heat.

### Experimentation

The experimental setup shown in Fig.4, consists of a cylindrical combustion chamber of mild steel of 1000 mm length, 206 mm outer diameter, and of 3 mm thickness, referred to as Drum. The drum is given an inclination of 12° for the movement of the fuel from one end to the another. The combustion chamber is made to oscillate because it makes the combustion of fuel more effectively by churning the fuel with the help of strips welded axially along of circumference inside the drum. The metal strips are provided inside the drum in the furnace region. These are fixed at 90° spacing along the circumference of the drum covering the entire axial length of the drum. In accordance with the constraints of fabrication, these strips could be welded to the drum only at two extremities thereby, leaving some air gap between strips and drum. This gap acts as contact resistance. Hence, the conduction of heat through these strips to the drum surface can be neglected. Because of the churning action, the fuel gets fully exposed to combustion from all sides helping in a satisfactory combustion process contributing to the rise in the combustion efficiency of the system. Also, the tilt angle given to the drum helps to convey the fuel from one end to the other end, obviating the use of additional fuel conveying mechanism, and therefore saves the cost. An oscillatory motion is imparted to the drum using chain drive, one sprocket is mounted on the drum rod and another is mounted on the motor shaft. D.C. motor with on/off control is used which can have a bi-direction rotation to obtain the rotation of the drum through a specific angle.

The fuel such as wood pieces, charcoal, etc. can be burned inside the drum although it is designed primarily for combusting bagasse. A helical coiled copper tube of a total of 9 turns, having 9.5 mm outer diameter and 0.5 mm thickness is brazed circumferentially over this drum. The working fluid, water is passed through this helical coil. A flexible joint is used at the inlet and the outlet of this helical pipe to enable a smooth rotary motion of the drum. The drum is connected to hollow pipes, as shown in Fig. 5, on both sides with the help of three stripes mounted in between shaft and drum. The shaft is housed in the bracket on both ends of the drum. The advantages of this type of combustion are the simplicity in design and manufacturing and ensure a smooth process. Also, the cooling of the shaft is not required as the flow of water is taken through the shaft at the inlet and discharged at the outlet.

The performance evaluation of the present system is presented in terms of the rise in temperature of water flowing through the tube, heat absorbed by water i.e. heat output of the system, and the thermal efficiency of the system. The experimental test was carried out at different mass flow rates from 0.2 lpm to 0.7 lpm, over a stationary and rotating

drum at different speeds of rotation from 2 to 8 rpm. Three thermocouples each at the inlet and outlet of the helical coil have been used for accurate temperature measurement. There were six thermocouples - three each on the bare drum surface and three at copper tube surface placed for the temperature measurements. The precision in drum speed rotation is maintained through a dedicated controller of the D.C. motor.

Initially, the experiments were performed on the stationary drum, and at Reynolds numbers ranging from 376 to 1372, especially near to the low and the high flow rate value the heating of the fluid is observed. Initially, ambient air temperature, initial drum, and copper tube surface temperatures were recorded. During the experimentation, at the steady-state inlet, and outlet, the mass of the fuel supply, and the time duration of the period of the test measurement were recorded. During the experimental run on the stationary drum, 150 gm of the fuel was used for a period of 406 seconds ensuring satisfactory combustion for each run.

The experiments were conducted on a rotating drum to observe the effect of turbulence on heat transfer. The set of experiments can be called as trials at a constant speed and variable flow rates. The speed of the drum selected is in the range of 2, 4, 6, and 8 rpm. The water flow rates between 0.2 to 0.7 lpm were recorded, corresponding to the Reynolds number range of 401 to 1724. At these flow conditions, the pressure drops were estimated as per the procedure mentioned in section 2.1. For each test run, the following parameters were calculated.

Temperature rise ( $\Delta T$ ) of water during the flow through the helical coiled tube,

$$\Delta T = T_o - T_i \quad (1)$$

Heat gained by the water,  $Q_w$  during the flow through the helical coiled tube,

$$Q_w = \dot{m} \cdot C_p \cdot \Delta T \quad (2)$$

Heat supplied by the fuel,  $Q_s$  during the test measurement period of 406 seconds,

$$Q_s = \frac{m_f \cdot CV}{t} \quad (3)$$

Thermal efficiency of the system,  $\eta$

$$\eta = \frac{Q_w}{Q_s} \quad (4)$$

The total heat supplied by fuel is utilized to raise the temperature of the drum, copper tube from initial ambient temperature values, and to heat the water flowing through the helical copper tube.

Heat utilized for raising the temperature of the drum of mass,  $m_d$  from the initial value,  $T_{id}$  to a surface temperature  $T_{sd}$ ,  $Q_d$ ,

$$Q_d = m_d C_{Pd} (T_{sd} - T_{id}) \quad (5)$$

Heat utilized for raising the temperature of the copper tube of mass,  $m_c$  from the initial value,  $T_{ic}$  to steady-state surface temperature  $T_{sc}$ ,  $Q_c$ ,

$$Q_c = m_c C_{Pc} (T_{sc} - T_{ic})$$

An energy balance between the total heat supplied and the heat utilized in the different parts of the system was made using the equation,

$$Q_s = Q_w + Q_d + Q_c + Q_{exhaust} \quad (7)$$

The heat energy,  $Q_{exhaust}$  was unutilized energy of exhaust hot flue gases, and its percentage varies from 70.10 to 81.63% of total heat supplied during all the experimental runs studied.

The mass of bagasse is measured by the calibrated electronic weighing machine which has a precision of 10 g. The flow rate of water through the helical pipe is measured manually by recording time in seconds for collecting 0.5 liters of water in a measuring jar. This process of measurement is repeated thrice, and average readings are taken to ensure the correctness of the measurement. The calibrated thermocouples used for temperature measurements have a standard deviation of 0.5°C with the measured value.

### Estimation Of Pressure Drop For Helical Pipe

Grindley and Gibson [13] first reported the experimental study for the flow of air through the helical coiled pipe. The authors reported that for the turbulent flow of air through a helical pipe, the frictional resistance was independent of the pressure of the fluid through the pipe and was proportional to the average fluid velocity. The authors formulated the law for variation of frictional resistance with temperature. Eustice [16] was next to report similar results for the flow of water through the flexible coiled tubing. The author concluded that increased flow velocities due to curved fluid flow increases the rise in flow resistance and hence, pressure losses. However, the theoretical analysis for the flow of incompressible Newtonian fluids confirming the experimental observations was reported by Dean [17]. The author reported a dynamically similar parameter,  $K_d$  which characterizes the flow in a torus at small flow rates. The square root of half of  $K_d$  was termed as a Dean number ( $De$ ).

$$De = Re \sqrt{\frac{d}{D}} \quad (8)$$

In the present experimental study, the entire flow range of water through the helical coiled tube was observed to be in the laminar flow regime globally. Therefore, the correlations for pressure drop reported in the literature were reviewed for this flow regime in curved tubes. Most of the available correlations for helical tubes are in the form of the ratio of fanning friction factor for curved tube ( $f_c$ ) to fanning friction factor for the flow of same fluid in a straight length of same diameter tube ( $f_s$ ). The physical significance

**Table 1.** Pressure drop correlations for curved tubes available in the literature

Authors (year)	Correlation	Operating conditions
White's correlation [18] (1929)	$\frac{f_c}{f_s} = \frac{1}{1 - [1 - (11.6/De)^{0.45}]^{2.22}}$	$D/d = 15.5, 50, 2050$ & $11.6 < De < 2000$
Adler's correlation [19] (1934)	$\frac{f_c}{f_s} = 0.1046 \sqrt{De}$	$De > 11.6$
Prandtl's correlation [20] (1949)	$\frac{f_c}{f_s} = 0.37(0.5De)^{0.36}$	$40 < De < 2000$
Ito's correlation [21] (1959)	$\frac{f_c}{f_s} = 21.5De / [1.56 + \log_{10} De]^{5.73}$	$13.5 < De < 2000$



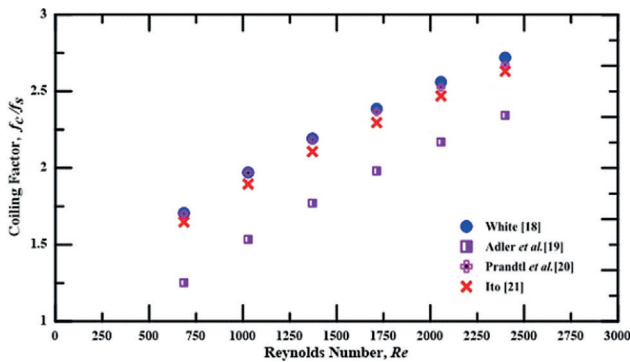


**Figure 6.** Variation of Coiling Factor,  $f_c/f_s$  with Reynolds number,  $Re$ .

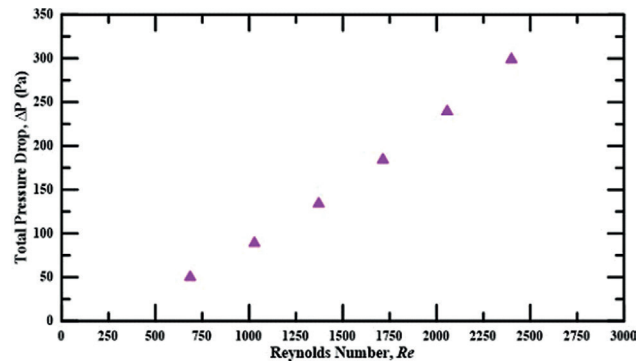


**Figure 7.** Variation of Total Pressure Drop,  $\Delta P$  with Reynolds number,  $Re$ .

**Table 2.** Summary of results for stationary system

Mass Flow Rate, $\dot{m}$ (kg/s)	Reynolds Number, $Re$	Rate of Fuel Consumption, $m_f$ (kg/s)	Temperature at Outlet, $T_{w(out)}$ (°C)	Temperature Rise of the Fluid, $\Delta T$ (°C)	Heat Output, $Q_w$ (W)	Thermal Efficiency of the System, $\eta$ (%)
0.002538	376	0.000369	61.6	39.6	421.3	12.67
0.002941	436	0.000369	60.9	38.9	479.0	14.41
0.003472	515	0.000369	45.1	23.1	335.8	10.10
0.009259	1372	0.000369	34.3	12.3	476.8	14.34

of friction factor ratio,  $f_c/f_s$  i.e. coiling effect factor ( $C$ ) lies in its equivalence to the ratio of pressure gradients in the coiled tube to that in the corresponding straight tube at the same flow rate. The critical Reynolds number for flow through coiled tube depends on the coil and tube diameter and is observed to be much higher than the same in straight tube i.e. 2300 [4]. The studies on the pressure drop in a helical coiled tube by various researchers were used in the present work for the estimation of pressure drop. It is observed that the coiling factor,  $C$  is expressed as a non-linear function of Dean Number,  $De$ .

The fanning friction factor for a straight tube in a laminar flow region is

$$f_s = \frac{16}{Re} \quad (9)$$

Friction factor for coil tube,  $f_c$  calculated using correlations mentioned in Table 1, along with Eq.(9). The ratio of friction factor i.e. coiling factor,  $f_c/f_s$  is observed to be similar with all correlations with small variations as shown in Fig.5. It is observed that there is an increase in the friction factor ratio with the increase in Reynolds number and as a conservative estimate the ratio predicting higher values.

In Fig.6, the coiling factor values predicted by White [18] correlation indicate slightly higher than predicted by

other investigators. Therefore, to remain on the conservative side, it is considered in the calculation of frictional pressure drop of flow through the helical coil tube configured in the present system.

$$(\Delta P)_{friction} = \frac{f_c}{4} \cdot \frac{\eta \cdot \pi D}{d} \cdot \frac{\rho \cdot u^2}{d} \quad (10)$$

The frictional pressure drop in a flow-through helical tube is computed using Eq. (10). Also, in addition to these major losses, minor losses due to small bends at the entry and exit of the helical tube were considered as follows:

$$(\Delta P)_{minor} = \frac{1}{2} \cdot k \cdot \rho \cdot u^2 \quad (11)$$

In the present experimental setup, for better estimation of minor losses, two bends were considered, and the value of loss coefficient,  $k$  was assumed to be equal to 1.0 [22]. The total pressure drop in the flow through the fluid flow system was expressed as,

$$\Delta P = (\Delta P)_{friction} + (\Delta P)_{minor} \quad (12)$$

The total pressure drop through the helical coiled tube was estimated using Eq. (12), shown in Fig.7 for different values of Reynolds number used during the present experimental study. Recognizing the results obtained using Eq.

(12), the pressure at the inlet of the helical coiled tube was maintained to a value of  $1.7 \times 10^5$  Pa using an overhead water storage tank.

**RESULTS AND DISCUSSION**

The performance parameters such as temperature at the outlet, temperature rise of the fluid, heat gained by water i.e. heat output, and efficiency of the thermal system, were computed at four different flow rates at stationary drum

conditions. The results for stationary and rotary systems are tabulated in Tables 2 and 3, respectively.

It is clear from Fig. 8 that there is a decrease in the temperature rise of fluid with the increase in Reynolds number for the same heat input to the system. At lower flow rates, the heat gained by the system is more than at higher flow rates. Fig. 8 also shows that the heat output of the system increases with an increase in Reynolds number.

Fig. 9 shows that there is an increase in thermal efficiency,  $\eta$  of the system from low to high Reynolds number

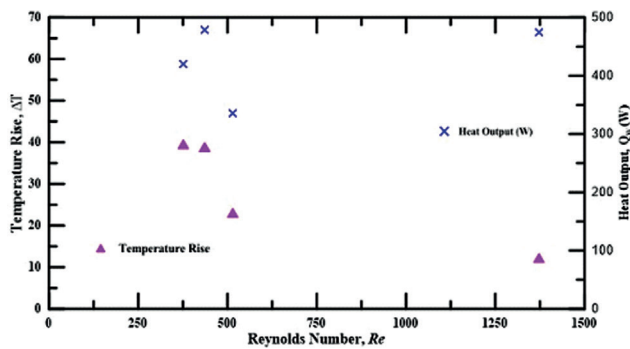


**Figure 8.** Variation of (a) Temperature Rise,  $\Delta T$  (b) Heat Output (W) with Reynolds number,  $Re$ .

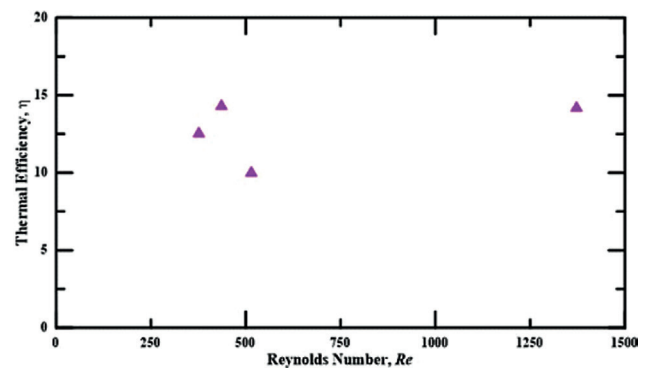


**Figure 9.** Variation of Thermal Efficiency,  $\eta$  with Reynolds number,  $Re$ .

**Table 3.** Summary of Results for Rotary System

Mass Flow Rate, $\dot{m}$ (kg/s)	Reynolds Number, $Re$	Speed of Rotation of Drum, $N$ (RPM)	Rate of Fuel Consumption, $\dot{m}_f$ (kg/s)	Temp. at Outlet, $T_{w(out)}$ (°C)	Temp. Rise of the Fluid, $\Delta T$ (°C)	Heat Output, $Q_w$ (W)	Thermal Efficiency of the System, $\eta$ (%)
0.0028	421	2	0.000369	53.4	31.4	373.50	11.2
0.0028	421	4	0.000369	56.2	34.2	406.81	12.2
0.0028	421	6	0.000369	58.3	36.3	431.19	13.0
0.0028	421	8	0.000369	65.3	43.3	514.45	15.5
0.0079	1176	2	0.000369	47.4	28.4	942.13	28.3
0.0079	1176	4	0.000369	57.7	38.7	1286.09	38.7
0.0079	1176	6	0.000369	64.3	45.3	1503.76	45.2
0.0079	1176	8	0.000369	61.8	42.8	1420.68	42.7
0.01064	1576	2	0.000369	38.1	16.1	717.12	21.6
0.01064	1576	4	0.000369	38.4	16.4	730.48	22.0
0.01064	1576	6	0.000369	40.3	18.3	812.88	24.4
0.01064	1576	8	0.000369	40.4	18.4	817.33	24.6
0.01163	1723	2	0.000369	34.9	15.2	740.03	22.3
0.01163	1723	4	0.000369	37.4	17.7	859.31	25.8
0.01163	1723	6	0.000369	43.2	23.5	1141.69	34.3
0.01163	1723	8	0.000369	44.0	24.3	1183.07	35.6

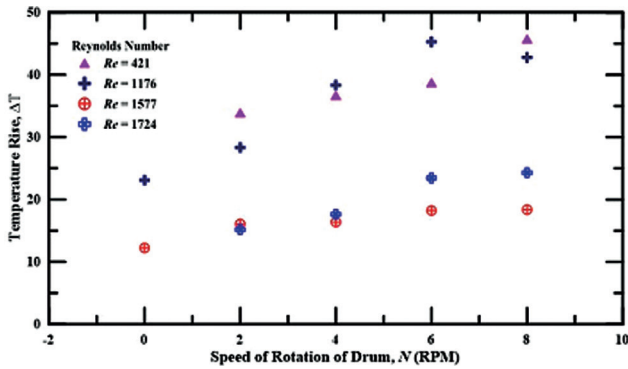


Figure 10. Variation of Temperature Rise,  $\Delta T$  with Speed of Rotation of Drum,  $N$  at Equal Reynolds number,  $Re$ .

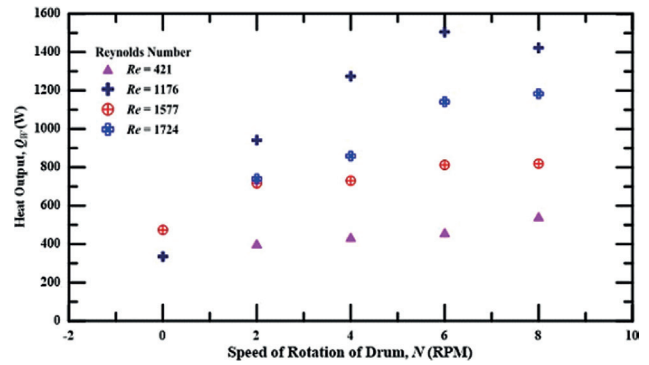


Figure 11. Variation of Heat Output,  $Q_w$  with Speed of Rotation of Drum,  $N$  at Equal Reynolds number,  $Re$ .

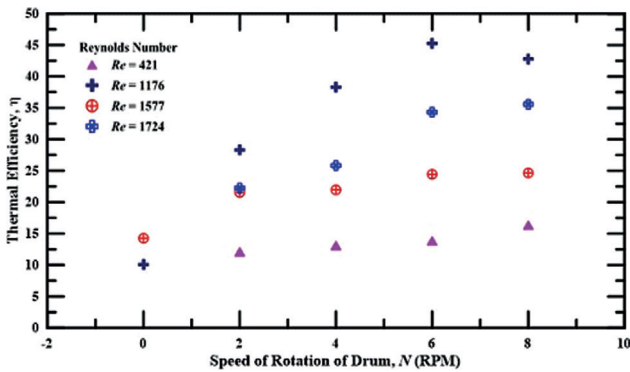


Figure 12. Variation of Thermal Efficiency,  $\eta$  with Speed of Rotation of Drum,  $N$  at Equal Reynolds number,  $Re$ .

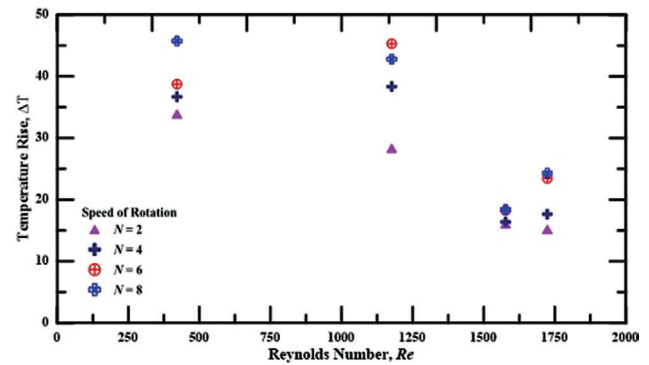


Figure 13. Variation of Temperature Rise,  $\Delta T$  with Reynolds number,  $Re$  at Equal Speed of Rotation of Drum,  $N$ .

due to better utilization of heat gained by the system at high flow rates.

The variation in temperature rise ( $\Delta T$ ) with the speed of rotation of drum ( $N$ ) at the same Reynolds number ( $Re$ ) is shown in Fig. 10. The data also includes the values at the stationary drum. It is observed that at a particular Reynolds number, there is a progressive increase in temperature rise,  $\Delta T$  of the fluid with the increase in drum rotation. This can be attributed to enhance local turbulence-induced due to the drum rotation. However, at a higher speed equal to 8 RPM, a slight decrease in temperature rise is observed at all Reynolds numbers except 421. It can be concluded that for Reynolds number more than 1176, there exists an optimum value of rotational speed,  $N$  equal to 6 for which the temperature rise is maximum. It can be also concluded that at the higher speed of rotation, the fluid through the helical coiled tube, due to large centrifugal force moves significantly away from the heated surface i.e. radially outward direction, restricting the interaction between the fluid and heat surface, and thereby reducing the temperature rise particularly for  $N$  equal to 8 RPM.

The variation of heat output,  $Q_w$  of rotating drum at different speeds of rotation, and also at stationary drum at same Reynolds number,  $Re$  is shown in Fig.10. The effect of temperature rise is reflected in the amount of heat output of the system; therefore, the same trend is observed for heat output as that of temperature rise. It can be concluded that the heat output of the system is maximum at the speed of rotation  $N = 6$  RPM.

The variation of thermal efficiency,  $\eta$  of rotating drum at different speeds of rotation, and at stationary drum at equal Reynolds number,  $Re$  is shown in Fig. 11. It is observed that at the stationary drum, there exists a routine path of the fluid through the helical coiled tube, causing lower thermal efficiency,  $\eta$  limited to 15%. However, when the rotation is imparted to the drum and subsequently to the helical coiled tube, additional turbulence is induced in the fluid, which causes more utilization of heat of combustion.

Therefore, there is a progressive rise in heat transfer to the fluid from hot flue gases with the increase in drum rotation from 2 to 6 RPM, and the thermal efficiency is observed to be maximum at the speed of rotation of the

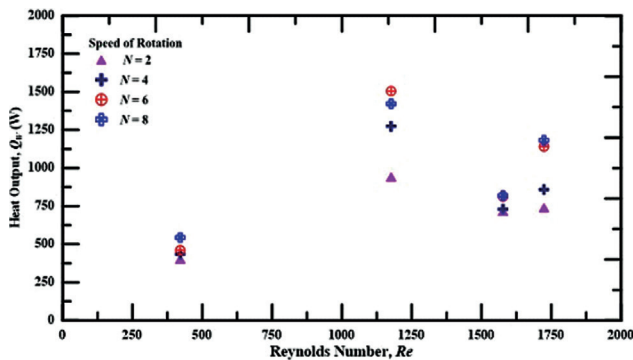


Figure 14. Variation of Heat Output,  $Q_w$  (W) with Reynolds number,  $Re$  at Equal Speed of Rotation of Drum,  $N$ .

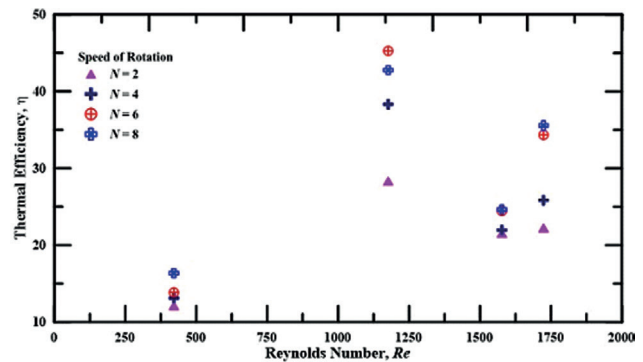


Figure 15. Variation of Thermal Efficiency,  $\eta$  with Reynolds number,  $Re$  at Equal Speed of Rotation of Drum

drum,  $N$  equal to 6 RPM. However, at higher speeds equal to 8 RPM, the efficiency remains almost constant for lower rotations equal to 4 and 6 RPM and reduces marginally at high rotations equal to 8 RPM. It can be concluded that the thermal efficiency variation also shows a similar trend of optimum speed equal to 6 RPM where thermal efficiency is maximum for Reynolds number more than 1000. At lower flow rates, a higher speed of rotation provides maximum heat transfer. It can be attributed to the fact that at Reynolds numbers, viscous forces dominate the inertial forces, however, due to high rotational speed, the reverse effect is likely to occur. Therefore, at lower flow rates, for maximum thermal efficiency higher speed of rotation favors as evident in Fig. 12. Therefore, it can be concluded that this system is efficient at the higher speed of rotation only at low flow rates equivalent to Reynolds number less than 1000.

The effect of flow rate i.e. Reynolds number,  $Re$  at equal speed of rotation of drum  $N$ , on performance measurement parameters is discussed in this section. The temperature rise of water with respect to Reynolds number is shown in Fig. 13. It is observed that till Reynolds number,  $Re$  equal to 1150, the temperature rise,  $\Delta T$  is almost same. At lower flow rates, the residence time of the fluid in the helical coiled tube is relatively more, which causes more heat gain during its travel from inlet to outlet of the tube, resulting in further temperature rise. However, this effect is not observed at higher flow rates, i.e. at Reynolds number more than 1150, there is a significant decrease in the temperature rise of the fluid. As the fluid moves rapidly through the tube, and due to the availability of limited time for heating, there exists a significant decrease in the temperature rise at a higher Reynolds number. At higher Reynolds numbers of 1750, and 1577, as shown in Fig. 13, it is observed that temperature rise is almost the same, and within the limits of experimental uncertainties.

The variation of heat output,  $Q_w$  of rotating drum at Reynolds number,  $Re$  at the equal speed of rotation,  $N$  is shown in Fig. 14. At a low Reynolds number, it is observed

that the heat output is less due to less value of mass flow rates through the tube, causes significantly less fluid mass responsible for heat gain. However, at higher flow rates, there exist a quick movement of fluid particles through the tube, and time available for transfer of heat to the fluid is not sufficient to obtain the required temperature rise.

Therefore, at both low and high flow rates, the heat output of the system is poor. Therefore, it can be concluded that the heat output of the present thermal system is more effective at a moderate range of Reynolds numbers from 1000 to 1250. The variation of thermal efficiency,  $\eta$  of the rotating system at different Reynolds numbers,  $Re$  at equal speed of rotation,  $N$  is shown in Fig. 15.

At lower Reynolds number  $Re$ , the heat gained by the water through the helical coiled tube is less, as a result the thermal efficiency,  $\eta$  of the system is found to be poor. At higher flow rates, it is observed that the heat gained by the fluid is moderate as discussed in the earlier part, the thermal efficiency,  $\eta$  marginally increases at Reynolds number  $Re$  equal to 1750. The Reynolds number range from 1000 to 1250, is observed to produce maximum thermal efficiency of 45%.

## CONCLUSION

The experimental work was carried out on bagasse-fired stationary, and rotary fluid heating combustion chamber with the flow of water through a helical coiled tube at four different flow rates correspond to the laminar regime. Various available correlations from the literature, best suited to the required flow regime were selected, and the correlation which predicts higher friction factor was used for calculation as a conservative estimation of pressure drop in the helical coiled tube. The experimental results indicate higher performance in terms of heat output, the thermal efficiency of the rotary condition than during stationary drum condition. It was observed that the rise in temperature increases, heat output, and thermal efficiency



increases with an increase in drum speed. The rising trends in the performance parameters are seen for all flow rates except at Reynolds number equal to 1120. There exists an optimum value of rotational speed equal to 6 rpm at which the thermal efficiency was found maximum. This trend was observed at all Reynolds numbers. The maximum temperature rise is observed to 45.3°C and the maximum thermal efficiency was observed to be 45.2 % at drum speed of 6 RPM at Reynolds number equal to 1176.

### Future Scope

In the present study, even though the bagasse is used as a solid fuel, other solid biomass can be tried. Also, the insulation over the drum can enhance the thermal efficiency of the system by restricting heat losses. However, with the use of insulations in the existing system overheating or loosening of brazed joints may occur. This difficulty can be addressed using advanced dissimilar metal joining processes. Another possibility of improvement in thermal efficiency will be the use of waste energy of hot flue gases to heat the raw bagasse before its supply to the combustion chamber to save energy. This can dry out bagasse improving its higher calorific value. Another aspect is about the flow rate of fluid through the helical pipe. In rural areas, due to the availability of lower flow rates / hydraulic heads, the present analysis is carried out under laminar flow conditions. The system can be tested for high flow rates i.e. in turbulent flow regime.

### NOMENCLATURE

CV	Lower calorific value of fuel (J/kg)
$\Delta P$	Pressure drop of fluid (N/m <sup>2</sup> )
D	Mean Diameter of the helical coil (m)
$d$	Inside diameter of helical wire coiled tube (m)
$\dot{m}$	Mass flow rate (kg/s)
n	Number of turns of helical coil
N	Speed of rotation of drum (RPM)
Q	Rate of heat transfer (W)
T	Temperature (K)
v	Average fluid velocity (m/s)
$C_p$	Specific heat at constant pressure (J/kg K)

#### Greek Symbols

$\rho$	Density of fluid (kg/m <sup>3</sup> )
$\mu$	Dynamic Viscosity (Pa s)

#### Subscripts

c	Curved tube
f	Fuel
o	Outlet of helical coiled tube
i	Inlet of helical coiled tube
s	Straight tube
t	Duration of test measurements (seconds)
w	Water

Dimensionless parameters

Re	Reynolds number, $\frac{\rho \cdot v \cdot D}{\mu}$
f	Average friction factor
De	Dean number,

### AUTHORSHIP CONTRIBUTIONS

Authors equally contributed to this work.

### DATA AVAILABILITY STATEMENT

The authors confirm that the data that supports the findings of this study are available within the article. Raw data that support the finding of this study are available from the corresponding author, upon reasonable request.

### CONFLICT OF INTEREST

The author declared no potential conflicts of interest with respect to the research, authorship, and/or publication of this article.

### ETHICS

There are no ethical issues with the publication of this manuscript.

### REFERENCES

- [1] Hugot E. Handbook of Cane Sugar Engineering. Amsterdam: Elsevier Science Publishers; 1986, pp. 919–960.
- [2] Berdowski JJM, Baas J, Bloos JPY, Visschedij AJH, Zandveld PYJ. The European emission inventory of heavy metals and persistent organic pollutants for 1990. Germany: U.S. Department of Energy Office of Scientific and Technical Information; 1997.
- [3] Sebastian T. Modern boiler types and applications, Energy Engineering and environmental protection publications. Steam Boiler Technology eBook: 2002. p. 2–15.
- [4] Pawel G. Types of incineration based on technological features. Amsterdam: Greenpeace International publication; 1995.
- [5] Reed LM, William A. Apparatus for the combustion of diverse material and heat utilization, Patent No.: 4724777, 1988.
- [6] Larson JB, Branscome JC. Rotating tire combustor. *US Patent, No.: US5967062, 1999.*
- [7] Mansell GE. Swivel base tilting rotary furnace. *US Patent, No.: US6676888B2, 2004.*
- [8] Swithenbank J. Rotatable fluidized bed incinerator. *US Patent, No.: US 6220189B1, 2001.*

- [9] Tantekin A, Özdil NF. Thermodynamic analysis of a fluidized bed coal combustor steam plant in textile industry. *J Therm Eng* 2017;3:1607–1614. [\[CrossRef\]](#)
- [10] Mehrabian R, Shiehnejadhesar A, Scharler R. Application of numerical modelling to biomass grate furnaces. *J Therm Eng* 2015;1:550–556. [\[CrossRef\]](#)
- [11] Sai Varun V, Tejesh P, Prashanth BN. Design and development of tilting rotary furnace, OP Conference Series: Materials Science and Engineering, Volume 310, International Conference on Advances in Materials and Manufacturing Applications (IConAMMA-2017) 17–19 August 2017, Bengaluru, India 2018;310:012–084. [\[CrossRef\]](#)
- [12] Jolibois N, Aleksandrov K, Hauser M, Stapf D, Seifert H, Matthes J, et al. Analysis of oscillating combustion for NO<sub>x</sub> reduction in pulverized fuel boilers. *MDPI Inventions*, 2021;6:9. [\[CrossRef\]](#)
- [13] Ali S. Pressure drop correlations for flow through regular helical coil tubes, *J Fluid Dyn Res* 2001;28:295–310. [\[CrossRef\]](#)
- [14] Hardik BK, Baburajan PK, Prabhu SV. Local heat transfer coefficient in helical coils with single phase flow. *Int J Heat Mass Transf* 2015;89:522–538. [\[CrossRef\]](#)
- [15] Grindley JH, Gibson AH. On the frictional resistance to the flow of air through a pipe. *Proc Royal Soc Lond* 1908;80:114–139. [\[CrossRef\]](#)
- [16] Eustice J. Flow of water in curved pipes. *Proc Royal Soc Lond* 1910;84:107–118. [\[CrossRef\]](#)
- [17] Dean WR. Note on the motion of fluid in curved pipe. *Philos Mag* 1927;20:208. [\[CrossRef\]](#)
- [18] White CM. Streamline flow through curved pipes. *Proc R Soc Lond* 1929;64:123–138. [\[CrossRef\]](#)
- [19] Adler M. Stromung in gekrumnten rohren. *Z Angew Math Mech* 1934;14:257–275. [\[CrossRef\]](#)
- [20] Prandtl L, Stromungslehre FD. *Essentials of Fluid Dynamics*. London: Blackie and Son; 1954.
- [21] Ito H. Friction factor for turbulent flow in curved pipes. *J Basic Eng Trans ASME* 1959;81:123–132. [\[CrossRef\]](#)
- [22] Idel' chik IE, Fried E. *Handbook of Hydraulic Resistance*. Washington: Hemisphere Publishing Corporation; 1986.